

INFLUENCE OF CEMENTATION PROTOCOL ON COLOR CHANGE AND FRACTURE RESISTANCE OF LITHIUM DISILICATE AND ULTRA-TRANSLUCENT ZIRCONIA LAMINATE VENEERS (IN-VITRO STUDY)

Samaa Nagy Kotb* and Hayat Ibrahim Mahrous El Banna*

ABSTRACT

Objective: To evaluate color change and fracture resistance of ultra-translucent zirconia (KATANA UTML) versus lithium disilicate (IPS e.max CAD) laminate veneers when cemented using preheated resin composite versus adhesive resin cement.

Materials and Methods: Forty-four standardized laminate veneers (0.5mm labial, 1.5mm incisal thickness) were fabricated using CAD/CAM technology and divided into four groups (n=11): ZH (ultra-translucent zirconia + preheated resin composite), ZA (ultra-translucent zirconia + adhesive resin cement), LH (lithium disilicate + preheated resin composite), and LA (lithium disilicate + adhesive resin cement). Specimens were cemented to epoxy resin dies following standardized surface conditioning protocols. Color measurements were performed using spectrophotometry (CIE Lab* system), and fracture resistance was tested using universal testing machine at 135° loading angle until failure, and failure modes were inspected under stereomicroscope.

Results: All groups exceeded clinical acceptability threshold for color change ($\Delta E > 3.3$), with ZH group exhibiting highest mean color change (16.30 ± 1.61) and ZA group demonstrating lowest (7.80 ± 1.77). Fracture resistance showed statistically significant differences between groups, with LH group achieving highest values (186.26 ± 27.43 N) and ZA group lowest (68.41 ± 8.44 N). Failure mode analysis revealed predominantly adhesive failures in ZA group (100%) versus mixed failures in preheated composite groups.

Conclusion: Material and cementation protocol influenced laminate veneer performance. All experimental groups exceeded clinically acceptable color change thresholds. Adhesive resin cement demonstrated superior color stability compared to preheated composite across both ceramic systems. For fracture resistance, lithium disilicate consistently outperformed ultra-translucent zirconia, with preheated composite providing mechanical enhancement.

KEYWORDS: Katana Ultratranslucent Monolithic Zirconia, IPS e.max CAD, preheated composite resin, adhesive resin cement, Failure Mode

* Lecturer of Fixed Prosthodontics, Faculty of Dentistry, Cairo University

INTRODUCTION

Laminate veneers have revolutionized esthetic dentistry by providing minimally invasive solutions for anterior teeth restorations (El Sayed et al., 2016; Aldafeeri et al., 2019). The success of these restorations depends to a great extent on achieving perfect color match and adequate mechanical properties to withstand functional loads (Zarone et al., 2019). Traditional porcelain veneers, while offering excellent optical properties and translucency, have been limited by their mechanical drawbacks, especially in thin sections, limiting their clinical applications (Burke et al., 2012; Rosentritt et al., 2015; Monteiro et al., 2018).

Innovations in dental CAD/CAM systems and materials have introduced ultra-translucent zirconia as a viable substitute to well established lithium disilicate glass ceramics (Miyazaki et al., 2009; Coldea et al., 2013). Contemporary Ultra-translucent zirconia systems as KATANA UTML (Kuraray Noritake) represent one of the latest generations of translucent ceramics, offering superior mechanical performance while achieving remarkable optical properties (Yıldız et al., 2024). The composition of KATANA UTML incorporates by approximation 7.55 wt% yttrium (equivalent to 5.4 mol% Y-PSZ [Yttria-Partially Stabilized Zirconia]), representing a substantial increase compare to conventional zirconia, resulting in improved translucency through increased cubic phase content while preserving adequate strength (Zhang et al., 2019).

The achievement of enhanced optical properties in Ultra-translucent zirconia could be attributed to increasing the yttria content (4-7.55 mol% Y_2O_3), reducing the grain size, and eliminating light-scattering defects (Gracis et al., 2015; Zhang et al., 2019). Nevertheless, the enhanced translucency comes with a compromise in mechanical properties, as ultra-translucent zirconia demonstrates reduced flexural strength (650-750 MPa) in comparison to conventional zirconia (>1000 MPa),

while maintaining superiority over lithium disilicate glass ceramic (300-450 MPa) (Bomicke et al., 2017; Kwon et al., 2018).

Lithium disilicate glass ceramics have achieved widespread clinical application in esthetic laminate veneer applications based on their superior optical properties and comparatively adequate mechanical properties (Gracis et al., 2015). The widespread reliability on CAD-CAM technology has made achievable the development of millable ceramic blocks for automated fabrication systems, as IPS e.max CAD ((Fasbinder et al., 2010).

The cementation protocol influences to a great extent both the color stability and mechanical performance of laminate veneers (Peumans et al., 2000). The substrate color, laminate veneer thickness, shade, and type of resin cement are all variables that contribute to the final restoration appearance (Chen et al., 2015; Hoorizad et al., 2021). Furthermore, the adhesive bonding technique impacts retention, fracture resistance, and reduces microleakage potential (Coelho et al., 2017).

Laminate veneers necessitate strong adhesive bonding protocols for ensure clinical longevity. The well established method for glass ceramics surface conditioning employs hydrofluoric acid (HF) etching followed by silane coupling agent application (Vichi et al., 2021; Ramos et al., 2022;), while light-activated resin cements are frequently preferred over dual-polymerizing systems due to their handling properties and enhanced bond strength (Yilmaz et al., 2012). However, materials presenting adhesive challenges such as ultra-translucent zirconia require MDP (10-Methacryloyloxydecyl Dihydrogen Phosphate)-containing primer systems and specific surface treatment protocols to establish reliable bonding interfaces. (Liu et al., 2022).

The use of preheated composite resin for cementation constitute an alternative strategy to enhance the physical and mechanical properties of the luting agent (Daronch et al., 2005; Fróes-

Salgado et al., 2010). Preheating composite resin within 37°C to 68°C temperature range substantially reduces its viscosity, optimizing flowability and interfacial adaptation to prepared tooth and restoration surfaces (Mundim et al., 2010; Deb et al., 2011;). Contemporary studies have shown that preheated composite demonstrate enhanced mechanical performance when compared to room-temperature application (Blalock et al., 2006; Rickman et al., 2011).

Spectrophotometric evaluation of color changes provides standardized measurement protocols, quantitative color expression, and enhanced precision (Paravina et al., 2015). Results are reported in the CIE Lab* system where L* measures brightness, a* measures red-green content, and b* measures yellow-blue content, which are collectively used for calculating ΔE (color changes) (Johnston, 2009). Color differences exceeding 3.3 ΔE units are considered clinically unacceptable and may require restoration replacement (Ghinea et al., 2010).

Fracture resistance represents fundamental parameter influencing laminate veneer clinical performance, with mechanical failure constituting the primary cause of restoration replacement in clinical settings. Extended clinical follow-up studies indicate that over a 15-year performance period, 67% of total laminate veneer failures are attributed to fracture (Dumfahrt et al., 2000; Beier et al., 2012). The mechanical performance of ultra-thin laminate veneers presents particular challenge, as reduced material thickness compromises inherent strength characteristics, while simultaneously increasing dependence on adhesive reinforcement from the supporting tooth structure (Yildiz et al., 2024).

The complex interaction among ceramic material selection, surface conditioning protocol, and luting agent composition creates a complex multivariable decision matrix that necessitate evidence-based protocol selection rather than universal implementation of conventional techniques.

Understanding these material-specific behavioural pattern is crucial for optimizing both esthetic and mechanical treatment outcomes in contemporary laminate veneer practice.

This study aimed to investigate whether ultra-translucent zirconia laminate veneers demonstrate color stability and fracture resistance comparable to lithium disilicate glass ceramic veneers when using different cementation protocols.

The null hypotheses tested were that ultra-translucent zirconia laminate veneers (KATANA UTML) and lithium disilicate glass ceramic (IPS e.max CAD) would show no significant differences in color change and fracture resistance when cemented with either preheated composite or adhesive resin cement, and that failure modes would be independent of treatment protocol.

MATERIALS AND METHODS

Study Design and Sample Size Calculation

This in vitro study was designed to evaluate and compare the influence of cementation protocol on color change and fracture resistance of ultra-translucent zirconia and lithium disilicate glass ceramic laminate veneers. Sample size was calculated according to power analysis using fracture resistance (N) as the primary outcome. Results of (Abdel-Nabi et al. 2020) showed that the mean value for Katana UTML zirconia group was 183.437 ± 25.77 N. Twenty N was the estimated mean difference between lithium disilicate and UTML zirconia groups, which was considered clinically meaningful based on the minimum loads required for normal masticatory function. Using alpha (α) level of (5%) and Beta (β) level of (20%) i.e., power = 80%; the minimum estimated sample size was 11 restorations per group with a total of 44 restorations.

Sample size calculation was done using PS program (Power and Sample Size Calculations Version 3). The selected effect size of 20 N

represents a clinically significant difference that would influence treatment protocol selection in clinical practice.

Study Groups

The specimens were divided into four groups (n=11) according to the restorative material and cementation protocol:

Group LA (Control): Lithium Disilicate Glass ceramic laminate veneers cemented by Adhesive resin cement

Group LH: Lithium Disilicate Glass ceramic laminate veneers cemented by preheated resin composite

Group ZA: Ultra-Translucent Zirconia laminate veneers cemented by Adhesive resin cement

Group ZH: Ultra-Translucent Zirconia laminate veneers cemented by preheated resin composite

Tooth Preparation

A maxillary right central incisor acrylic tooth of a typodont model (NISSIN Dental Model, Koyota, Japan) was selected to be prepared and serve as a die. A silicon putty index was obtained using addition silicon material (PANASIL, Putty Soft Kettenbach dental-Germany) before reduction. A butt-joint incisal preparation design was chosen to reduce the incisal edge by 1 mm using a wheel stone grit green band (Frank, Germany). Labially depth grooves were obtained using 0.3 and 0.5 depth cutter diamond stones (Frank, Germany) in two planes. The required amount of preparation was done using tapered diamond stone with a round end and grit blue band (Frank, Germany) to obtain chamfer finish line 0.3-0.4mm thickness and 0.5mm supragingivally. Mesial and distal boundaries were about 1 mm to mesio and distobuccal line angles, just before contact point. Finishing diamond stones were used to finish the tooth and the putty index section was used to ensure the required reduction.

Then polishing of the preparation was done using polishing brush and paste.

Digital Impression and Restoration Design

The prepared typodont tooth was digitized using an intraoral scanner "Medit i500 intraoral scanner (Medit Corp., Seoul, Korea)". The scanning procedure was performed according to the manufacturer's recommendations to obtain a high-quality digital impression. The designing phase of the veneers was completed using exoCAD dentalCAD software (exocad GmbH, Darmstadt, Germany), where a standardized veneer design was created with a uniform thickness of 0.5 mm at the labial surface and 1.5 mm at the incisal edge. The cement gap was set at 50 μ m and 1 mm away from the margins for all specimens to standardize the designed internal gap. Laminate veneer restoration shape was determined by using the contralateral tooth as a reference using the copy then mirror option. The same digital design file was used for fabricating all specimens to eliminate design variables from the study.

Fabrication of Laminate Veneers

Lithium Disilicate Glass Ceramic Veneers

For Groups LA and LH, lithium disilicate glass ceramic blocks (IPS e.max CAD, Ivoclar Vivadent, Schaan, Liechtenstein) were used. The blocks were secured in the milling machine (inLab MC XL, Dentsply Sirona, York, PA, USA). Specimens were milled as recommended by the manufacturer.

Following the milling procedure, the lithium disilicate veneers were carefully removed from the blocks. The attachment sprue was removed using fine-grit diamond burs under water cooling. IPS e.max CAD Crystal/Glaze Paste (Ivoclar Vivadent, Schaan, Liechtenstein) was applied evenly on the blue stage. The specimens were then crystallized in a ceramic furnace (Programat P310, Ivoclar Vivadent, Schaan, Liechtenstein) according to the manufacturer's recommended crystallization program.

Ultra-Translucent Zirconia Veneers

For Groups ZA and ZH, ultra-translucent zirconia discs (KATANA Zirconia UTML, Kuraray Noritake Dental Inc., Tokyo, Japan) were used. The discs were secured in the milling machine, and the same design file used for the lithium disilicate specimens was utilized. Specimens were milled as recommended by the manufacturer.

After milling, the zirconia veneers were carefully separated from the discs, and the attachment sprue was removed using fine-grit diamond burs. The specimens were sintered in a zirconia sintering furnace (inFire HTC speed, Dentsply Sirona, York, PA, USA) following the manufacturer's recommended sintering program (1550°C for 2 hours). Then, all zirconia veneers were glazed using a zirconia glaze "Apply CZR PRESS" (Kuraray Noritake Dental Inc., Japan) and fired using glaze cycles in the porcelain furnace "Programat CS3".

All specimens were inspected under 2.5× magnification to verify their integrity and absence of visible defects before evaluation. Each specimen was numbered and stored in individual labeled containers

Fabrication of Epoxy Resin Dies

Silicon molds for typodont teeth were made using duplicating addition silicon Material (Repisil 22 N Dent-e-Con e.K., Lonsee, Germany). The typodont

tooth was placed in the center of a cylindrical plastic container then addition silicon material was poured into the plastic container under vibration to prevent air entrapment, left in place for 30 minutes to set, and then the silicon mold was removed from the plastic container. The typodont die was duplicated from the silicon mold to get 44 replicas fabricated from epoxy resin material (Kemapoxy 150, CMB, Chemical modern building international, Egypt) [Figure 1]

Cementation of Laminate Veneers

The epoxy resin die surfaces were etched with 3M Scotchbond™ Etchant (3M Oral Care, St. Paul, MN, USA), a 37% phosphoric acid gel for 30 s, washed for 30 seconds under running water, and air-dried. A layer of adhesive (All-Bond Universal, Bisco Inc., Schaumburg, IL, USA) was applied then and light cured for 20 seconds using an LED light-curing unit (Guilin Woodpecker Medical Instrument Co., Ltd., Guilin, Guangxi, China).

The fitting surface of all lithium disilicate **Group (L)** laminate veneers were etched with Porcelain Etchant 9.5% Buffered Hydrofluoric Acid Gel (Bisco Inc., Schaumburg, IL, USA) for 20 seconds, rinsed off then cleaned in ultrasonic bath for three minutes and dried with air. Silane coupling agent (Bisco Inc., Schaumburg, IL, USA) was applied to the fitting surface of the veneer and allowed to dry for 60 seconds then dispersed to obtain a thin coat.

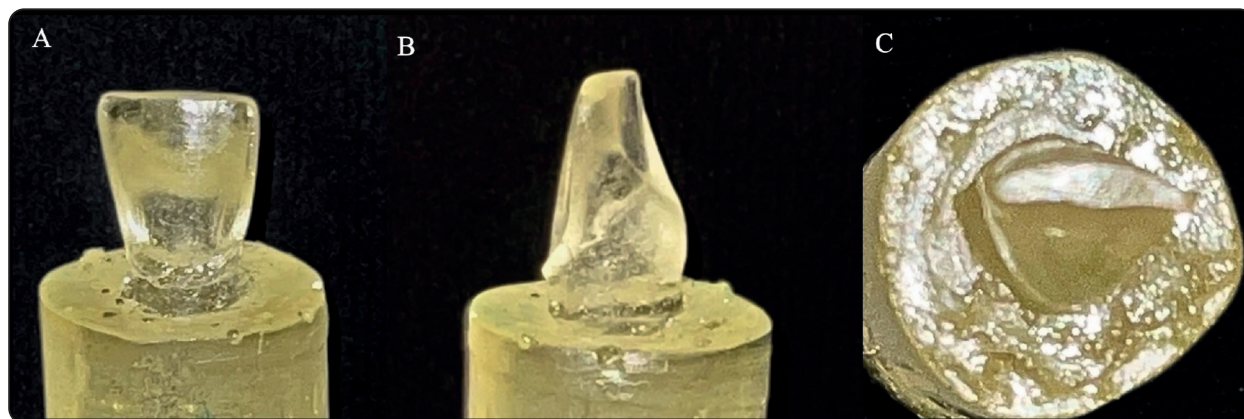


Fig. (1) Epoxy resin die (A) Labial view, (B) Proximal View, (C) Incisal view

The fitting surface of all ultra translucent monolithic zirconia **Group (Z)** laminate veneers were sandblasted with 30 µm silica-modified Al₂O₃ particles (CoJet, 3M ESPE, Seefeld, Germany) at 1-2 bar (0.1-0.2 MPa) pressure at 10 mm from the surface for 10-15 seconds, followed by (All-Bond Universal, Bisco Inc., Schaumburg, IL, USA) where a thin layer of adhesive was applied to the treated surface for 20 s with a microbrush, then air-dried for 5 seconds and light cured for 10 seconds using an LED light-curing unit (Guilin Woodpecker Medical Instrument Co., Ltd., Guilin, Guangxi, China).

For Groups LA and ZA

Veneer cementation was carried out using Choice 2 Light-polymerizing adhesive resin cement Translucent shade (Choice 2, Bisco Inc., Schaumburg, IL, USA) translucent shade was applied to the treated ceramic surface. The veneer was then positioned on top of the epoxy die under static finger pressure where tack curing for 2-4 seconds was carried out and excess luting agent was removed with a clean microbrush, and the specimen was then light polymerized for 1 minute using an LED light-curing unit (Guilin Woodpecker Medical Instrument Co., Ltd., Guilin, Guangxi, China) through the ceramic [Figure 2].

For Groups LH and ZH

Veneer cementation was performed using

Brilliant EverGlow nanohybrid composite Translucent shade (Coltene/Whaledent AG, Altstätten, Switzerland). Composite was preheated to 70°C using an AR Heat composite heater (24W, ±1°C precision) for 10 minutes prior to application. The heated composite was applied to the treated ceramic surface. The veneer was then positioned on top of the epoxy die under static finger pressure where tack curing for 2-4 seconds was carried out and excess luting agent was removed with a clean microbrush, and the specimen was then light polymerized for 1 minute using an LED light-curing unit (Guilin Woodpecker Medical Instrument Co., Ltd., Guilin, Guangxi, China) through the ceramic [Figure 3].

Color Change Test

Color of samples was measured before and after cementation to epoxy resin dies using digital spectrophotometer (Model RM200QC, X-Rite, Neu-Isenburg, Germany). The change in color (ΔE) values was evaluated through calculation of the difference in color measurements of all samples pre and post cementation by using the formula:

$$\Delta E = [(\Delta L^*)^2 + (\Delta a^*)^2 + (\Delta b^*)^2]^{1/2}$$

L* stands for lightness, **a*** for green-red and **b*** for blue-yellow. ΔL^* , Δa^* , Δb^* correspond to the differences before and after cementation of laminate veneers.

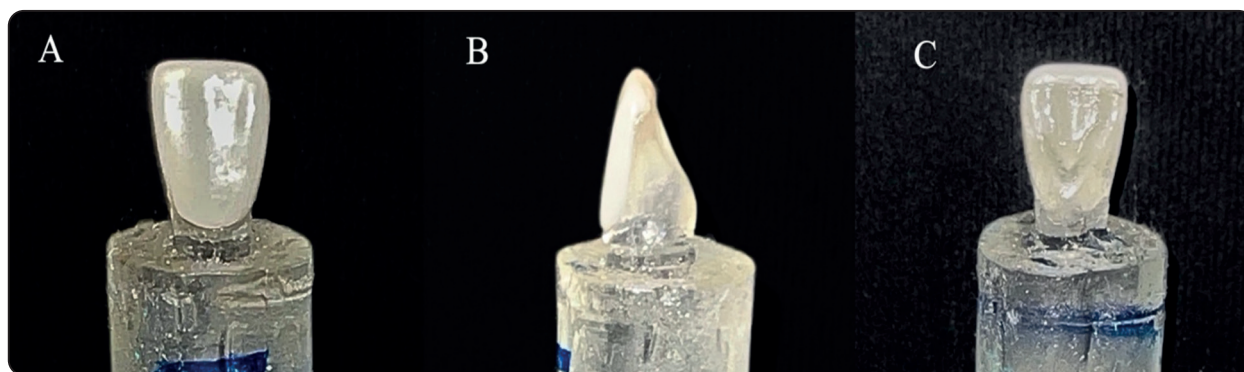


Fig. (2) Cemented Lithium Disilicate Laminate veneer (Group LA) on epoxy resin die (A) Labial View, (B) Proximal View, (C) Palatal View

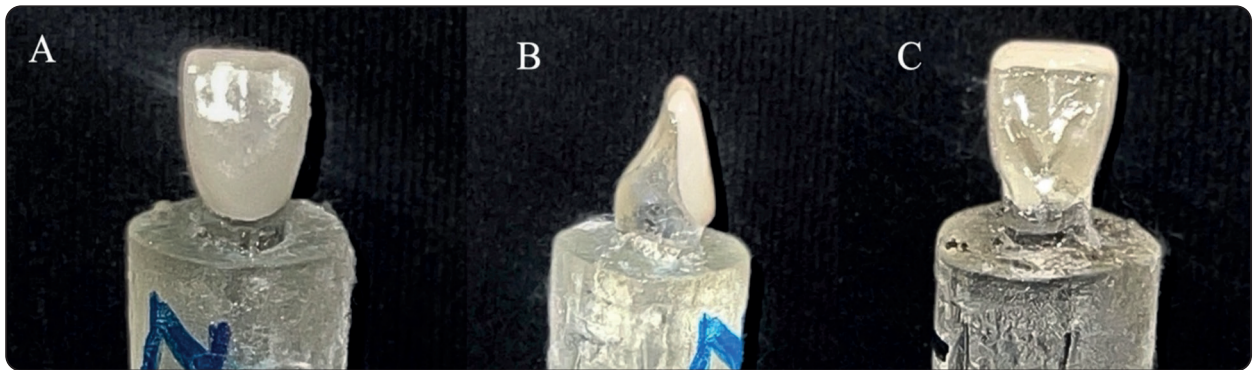


Fig. (3) Cemented Ultra Translucent Monolithic Zirconia Laminate Veneer (Group ZH) on epoxy resin die (A) Labial View, (B) Proximal View, (C) Palatal View

Fracture Resistance Test

Specimens were mounted in a universal testing machine (Instron 3345, Instron Co., Norwood, Massachusetts, USA) with a loadcell of 5kN and a 6 mm stainless steel ball positioned at an angle of 135° between the long axis of the steel block and the composite resin die (through housing the sample in the specially designed 45° angle jig) applying compressive load at 0.5 mm/min until failure. A polyethylene sheet ensured uniform stress distribution. Loading was applied to the incisal edge. Maximum loads were recorded in Newtons and converted to MPa using Bluehill Lite software (Instron® Bluehill Lite Software). [Figure 4]

Failure Mode Analysis

Fractured specimens were examined under stereomicroscope (SZ61, Olympus Corporation, Tokyo, Japan) at 20× magnification and classified as:

Statistical Analysis

Statistical analysis was performed with SPSS 27®, Graph Pad Prism® and Microsoft Excel



Fig. (4) Fracture resistance testing

2016. All quantitative data (color changes, fracture resistance) were presented as minimum, maximum, means and standard deviation (SD) value and explored for normality by using Shapiro Wilk Normality test and Kolmogorov test which revealed that all data were normally distributed.

TABLE (1) Classification of the failure mode

Failure Type	Description	Prognosis
Type I - Adhesive	Complete separation at cement-substrate interface	Favourable
Type II - Mixed	Combination of adhesive separation + substrate fracture	Unfavourable
Type III - Cohesive	Fracture through die material without separation	Unfavourable

Accordingly, comparison between different groups was performed by using One Way ANOVA test followed by Tukey's Post Hoc test for multiple comparisons. In qualitative data (failure mode) all data were presented as frequency and percentages, all comparisons were performed by using Fisher Exact test. The significant level was set at $P \leq 0.05$.

RESULTS

I. Color Change

The color change values (ΔE) for the four experimental groups — ZH, ZA, LH, and LA — are presented in Tables 2, 3 and Figure 5. A comparison between groups using a one-way ANOVA test revealed a statistically significant difference ($P = 0.0001$). According to the Tukey Post Hoc test, the ZH group exhibited the highest mean color change (16.30 ± 1.61). This was followed by the LH group (12.97 ± 3.87). The LA group (9.17 ± 1.34) and the

ZA group (7.80 ± 1.77) demonstrated comparatively lower color changes with insignificant difference between them.

II. Fracture Resistance

The fracture resistance values (in Newtons) across four experimental groups: ZH, ZA, LH, and LA were presented in Tables 4, 5 and Figure 6. A comparison between groups was performed by using One-way ANOVA test revealed a statistically significant difference between groups ($P = 0.0001$), followed by Tukey Post Hoc test which revealed that the mean fracture resistance was highest in the LH group (186.26 ± 27.43 N), followed closely by the ZH group (172.09 ± 17.84 N). The LA group demonstrated a moderate mean value of 155.81 ± 9.37 N, with insignificant difference between them, while the ZA group exhibited significantly the least mean fracture resistance at (68.41 ± 8.44 N).

TABLE (2) Color changes (ΔE) in all experimental groups (n=11 per group), comparison using One-Way ANOVA test

	Minimum	Maximum	Mean	Standard Deviation	P value
ZH	13.68	18.16	16.30	1.61	0.0001*
ZA	4.98	9.99	7.80	1.77	
LH	8.41	19.88	12.97	3.87	
LA	7.36	10.57	9.17	1.34	

*Significant difference as $P \leq 0.05$.

TABLE (3) Pairwise comparison regarding color changes in all groups

Pairwise comparison		Mean Difference	Std. Error	95% Confidence Interval		P value
				Lower Bound	Upper Bound	
ZH	ZA	8.49	1.01	5.78	11.21	0.0001*
ZH	LH	3.32	1.01	0.61	6.04	0.01*
ZH	LA	7.13	1.01	4.42	9.84	0.0001*
ZA	LH	-5.17	1.01	-7.88	-2.46	0.0001*
ZA	LA	-1.36	1.01	-4.08	1.35	0.54
LH	LA	3.81	1.01	1.09	6.52	0.0001*

*Significant difference as $P \leq 0.05$.

TABLE (4) Fracture resistance in all groups, comparison between them using One Way ANOVA test

Fracture resistance	Minimum	Maximum	Mean	Standard Deviation	P value
ZH	153.46	187.62	172.09	17.84	0.0001*
ZA	56.73	77.27	68.41	8.44	
LH	158.83	213.68	186.26	27.43	
LA	149.12	174.24	155.81	9.37	

*Significant difference as $P \leq 0.05$.

TABLE (5) Pairwise comparison regarding fracture resistance in all groups

Pairwise comparison		Mean Difference	Std. Error	95% Confidence Interval		P value
				Lower Bound	Upper Bound	
ZH	ZA	103.69	7.48	83.65	123.72	0.0001*
ZH	LH	-14.16	7.48	-34.20	5.88	0.25
ZH	LA	16.28	7.48	-3.76	36.32	0.15
ZA	LH	-117.85	7.48	-137.89	-97.81	0.0001*
ZA	LA	-87.40	7.48	-107.44	-67.37	0.0001*
LH	LA	30.44	7.48	10.41	50.48	0.0001*

*Significant difference as $P \leq 0.05$.

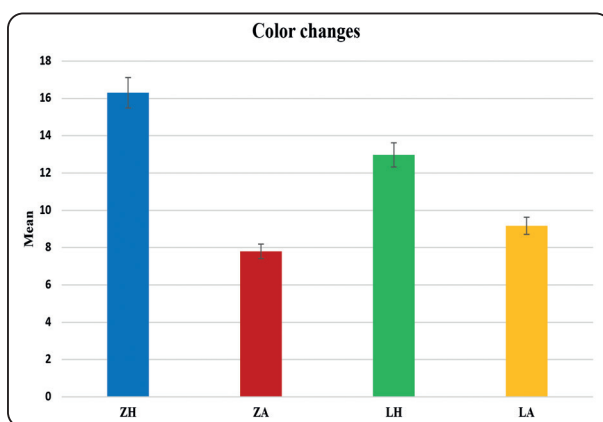


Fig. (5) Bar chart showing Color changes in all groups

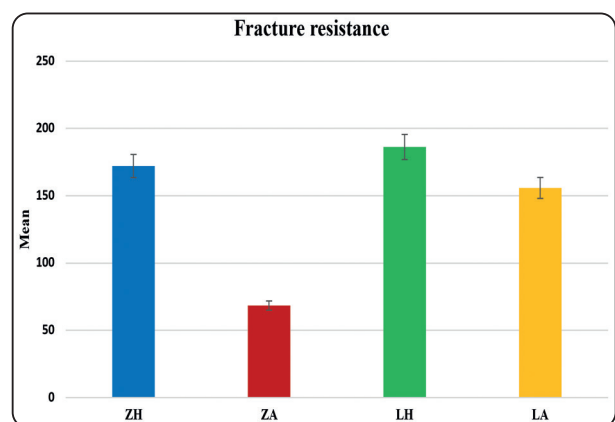


Fig. (6) Bar chart showing Fracture resistance in all groups

III. Failure Mode

The distribution of different types of failure modes — adhesive, mixed, and cohesive — among the four experimental groups is shown in Table 6 and Figure 7. A statistically significant difference in failure mode distribution was observed between groups ($P = 0.001$) by using Fisher's Exact test. In the ZH group, failure was predominantly

mixed (72.7%), with 27.3% adhesive failures and no cohesive failures. The ZA group showed exclusively adhesive failures (100%). The LH group demonstrated a more varied failure pattern, with 45.5% mixed, 27.3% adhesive, and 27.3% cohesive failures. In the LA group, failures were divided between adhesive (54.5%) and mixed (45.5%), with no cohesive failures reported.

TABLE (6) Distribution of different types of failure among all groups

Failure mode							P value
Adhesive			Mixed		Cohesive		
	Count	Row N %	Count	Row N %	Count	Row N %	
ZH	3	27.3%	8	72.7%	0	0.0%	0.001*
ZA	11	100.0%	0	0.0%	0	0.0%	
LH	3	27.3%	5	45.5%	3	27.3%	
LA	6	54.5%	5	45.5%	0	0.0%	

*Significant difference as $P \leq 0.05$.

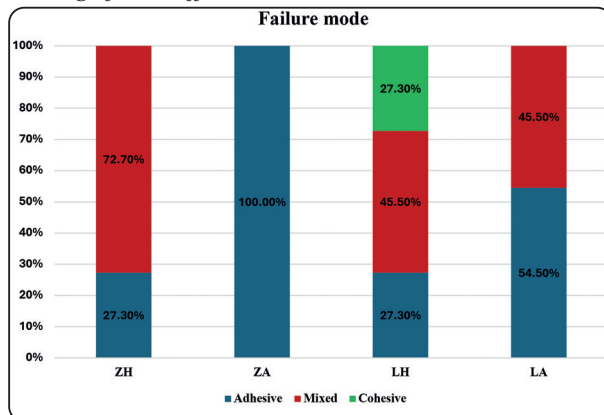


Fig. (7) Bar chart showing Distribution of different types of failure among all groups

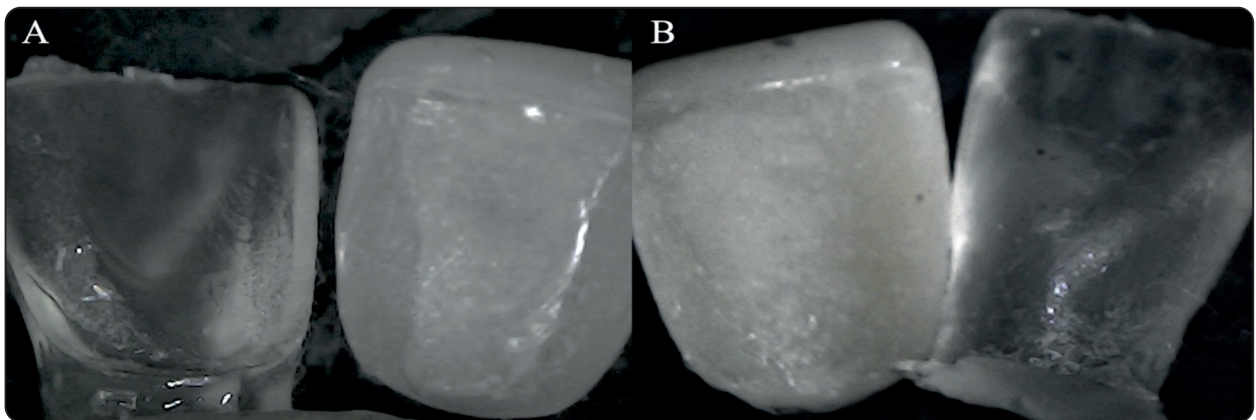


Fig. (8) Representative microscopic images of failure modes: (A) Adhesive fracture (Type I) of Group ZA (B) Mixed Fracture (Type II) of Group LH

DISCUSSION

This study evaluated the color change and fracture resistance of ultra-translucent zirconia (KATANA UTML) and lithium disilicate (IPS e.max CAD) laminate veneers using two different cementation protocols. Material type and cementation protocol significantly influenced veneer performance, with different factors dominating specific outcomes, thereby rejecting the null hypotheses.

KATANA UTML and IPS e.max CAD represent current state-of-the-art monolithic ceramics for anterior applications. KATANA UTML, with 7.55 wt% yttrium content (5.4 mol% Y-PSZ), offers enhanced optical properties while maintaining adequate mechanical strength (Zhang et al., 2019). IPS e.max CAD provides an established clinical benchmark with survival rates exceeding 90% at 10-year follow-up (Layton et al., 2013).

The standardized veneer design (0.5 mm labial, 1.5 mm incisal thickness) aligns with contemporary clinical practice and optimal performance ranges (Araujo et al., 2021; Malallah et al., 2022). Epoxy resin dies provided standardized substrate properties while eliminating biological variability (Soares et al., 2005; Malallah et al., 2022).

Surface conditioning followed established protocols: 9.5% hydrofluoric acid etching for lithium disilicate (Ramos et al., 2022) and tribochemical silica coating for zirconia (Li et al., 2024). Two cementation protocols were evaluated: light-polymerizing adhesive resin cement (Choice 2, Bisco) and preheated composite (Brilliant EverGlow, 70°C), representing current clinical approaches with different performance characteristics (Blalock et al., 2006).

Color measurement using digital spectrophotometry (CIE Lab* system) provided quantitative evaluation (Ghinea et al., 2010; Paravina et al., 2015;), while fracture resistance testing (135° loading, 0.5 mm/min) simulated physiological conditions, though acute loading does not replicate clinical fatigue patterns (Al-Ali et al., 2023).

In our study; All experimental groups exceeded contemporary clinical acceptability thresholds ($\Delta E > 3.3$), with values ranging from 7.80 ± 1.77 (ZA) to 16.30 ± 1.61 (ZH), indicating that 83.3-100% of specimens showed clinically perceptible color alterations (Ghinea et al., 2010). This finding demonstrates that current cementation protocols require optimization for optimal esthetic outcomes, particularly as substrate and cementing material have greater influence on ultra-thin ceramic veneers (≤ 0.5 mm thickness) (Pissaia et al., 2019).

Cementation protocol emerged as the dominant factor influencing color reproduction, with adhesive resin cement demonstrating superior performance compared to preheated composite across both ceramic systems. The ZA group achieved the lowest color change ($7.80 \pm 1.77 \Delta E$), while ZH showed the highest ($16.30 \pm 1.61 \Delta E$), representing a 109% increase with preheated composite cementation. This substantial difference aligns with recent systematic evidence demonstrating that preheated composite resins exhibit significantly greater color alterations than conventional resin cements (Caminha et al., 2022; Raposo et al., 2024).

The superior performance of adhesive resin cement can be attributed to higher concentrations of stabilizing additives and lower susceptibility to hydrolytic degradation compared to heated composite resins (Saati et al., 2021). Conversely, poor color stability of preheated composite systems may result from thermal-induced chemical modifications during heating, altering polymerization kinetics and increasing susceptibility to oxidative degradation (Gürdal et al., 2018).

Ultra-translucent zirconia demonstrated greater sensitivity to cementation method compared to lithium disilicate. The difference between ZA and ZH groups (109% increase) was substantially larger than between LA and LH groups (41.4% increase). This finding aligns with established principles where translucent zirconia's crystalline structure exhibits greater sensitivity to refractive index mismatches

with different luting agents (Zhang et al., 2018; Chen et al., 2024).

Lithium disilicate showed more moderate responses (LA: $9.17 \pm 1.34 \Delta E$ vs. LH: $12.97 \pm 3.87 \Delta E$), with the LA group positioning as an intermediate option demonstrating better color stability than preheated composite groups but greater change than the optimal ZA combination. The notable standard deviation (± 3.87) in the LH group indicates considerable variability, suggesting unpredictable color outcomes with preheated composite cementation (Kandil et al., 2019).

Recent studies confirm that ceramic material type significantly affects color stability, with high-translucent ceramics exhibiting greater color changes upon aging, and self-adhesive resin cements showing superior color stability (Saati et al., 2021; Chen et al., 2024).

Some studies reported more favorable outcomes. Le et al. (2019) found comparable color stability between translucent zirconia and conventional ceramics, though using different surface treatments and aging protocols. Vichi et al. (2020) reported ΔE values of 2.1-4.8 for ultra-translucent zirconia veneers, considerably lower than our findings, though without preheated composite protocols. These discrepancies may reflect differences in measurement protocols, specimen preparation, or material formulations (Harada et al., 2016).

The universal exceedance of acceptability thresholds may reflect: immediate post-cementation assessment potentially overestimating changes due to incomplete polymerization; epoxy substrate not replicating complex optical interactions of natural tooth structure; and standardized lighting conditions not representing typical clinical viewing environments.

The performance hierarchy (ZA < LA < LH < ZH) provides evidence-based guidance for protocol selection. The ZA protocol provides strong evidence that adhesive resin cementation should be preferred when color stability is the primary concern,

despite potential limitations in other performance parameters. The LH group's poor color stability ($12.97 \Delta E$) strongly argues against preheated composite cementation with lithium disilicate, as this combination fails to leverage the ceramic's inherent optical advantages.

The fracture resistance evaluation revealed significant material-dependent differences, with lithium disilicate demonstrating superior mechanical performance compared to ultra-translucent zirconia across both cementation protocols. The performance hierarchy was: LH ($186.26 \pm 27.43 N$) > ZH ($172.09 \pm 17.84 N$) > LA ($155.81 \pm 9.37 N$) > ZA ($68.41 \pm 8.44 N$).

Recent studies confirm that material thickness significantly influences fracture resistance of ceramic laminate veneers, with ultra-thin veneers ($\leq 0.5 mm$) demonstrating material-dependent load-to-failure values (Yildiz et al., 2024).

The superior fracture resistance of lithium disilicate groups (LH: $186.26 \pm 27.43 N$; LA: $155.81 \pm 9.37 N$) compared to ultra-translucent zirconia (ZH: $172.09 \pm 17.84 N$; ZA: $68.41 \pm 8.44 N$) aligns with established Contemporary comparative studies that have demonstrated that Lithium disilicate consistently demonstrates superior mechanical performance compared to other ceramic systems in thin-section applications (Al-Ali et al., 2023), and that lithium disilicate laminate veneers consistently exhibit superior load-to-failure values compared to monolithic zirconia veneers of equivalent thickness, with lithium disilicate showing enhanced resistance to fracture initiation (Yildiz et al., 2024). This mechanical advantage stems from lithium disilicate's needle-like crystal microstructure, which provides effective crack deflection mechanisms and superior fracture toughness in thin-section applications (Zarone et al., 2019).

The ZA group's critically inadequate performance ($68.41 \pm 8.44 N$) represents a significant clinical concern, falling well below the established minimum threshold of 100 N for anterior veneer applications.

Recent studies confirm that bonding effectiveness remains problematic for ultra-translucent zirconia, with debonding representing a primary failure mode (Guess et al., 2010; Chen et al., 2024).

Abdel-Nabi et al. (2020) reported fracture loads of 183.4 ± 25.8 N for KATANA UTML zirconia, higher than our ZH group findings. This discrepancy may reflect differences in surface treatment protocols, specimen geometry, or testing methodology (Conrad et al., 2007).

The remarkable improvement in fracture resistance with preheated composite cementation represents a significant finding. The ZH group demonstrated an 87.0% increase compared to ZA, while the LH group showed a 19.5% improvement over LA. This can be attributed to improved physical and mechanical properties of the luting agent. Preheating composite resin significantly reduces viscosity, improving flowability and adaptation to restoration surfaces (Deb et al., 2011). Studies demonstrate that preheated composite exhibits improved mechanical properties, including enhanced degree of conversion and marginal adaptation compared to room-temperature application (Daronch et al., 2005; Fróes-Salgado et al., 2010). Clinical evidence supports the long-term success of preheated composite cementation for laminate veneers (Marcondes et al., 2021).

The failure mode analysis provided crucial insights into bonding quality and mechanical behavior. The ZA group demonstrated exclusively Type I adhesive failures (100%), confirming inadequate ceramic-resin interface bonding. In contrast, groups employing preheated composite showed predominantly mixed failures (ZH: 72.7%, LH: 45.5%), suggesting adequate interfacial bonding with load transfer to the ceramic-substrate interface.

These findings align with established principles where adhesive failures indicate inadequate surface conditioning while mixed failures suggest optimal bonding characteristics (Van Meerbeek et al., 2010;

Thompson et al., 2011). The LH group's diverse failure pattern, including 27.3% cohesive failures within the substrate, indicates optimal mechanical performance within testing limitations.

Studies demonstrate that color stability depends on resin cement composition and its visibility through ceramic veneers (Hoorizad et al., 2021), while fracture resistance is significantly influenced by cementation mode and bonding effectiveness. Soares et al. (2005) confirms that ceramic material type requires different surface conditioning protocols: glass ceramics require hydrofluoric acid etching (5-10% for 60s) followed by silane application, while zirconia requires tribochemical silica coating with aluminum oxide particles.

The performance hierarchy (ZA < LA < LH < ZH for color; ZA < LA < ZH < LH for fracture resistance) reveals inherent trade-offs requiring clinical prioritization. No single protocol optimized all outcomes simultaneously. For esthetically critical cases, ZA protocol provides superior color stability despite mechanical limitations. For stress-bearing applications, LH protocol offers optimal fracture resistance despite color stability concerns.

This in-vitro analysis has inherent limitations. The use of epoxy dies, while providing standardized evaluation conditions, may not fully replicate the complex mechanical and thermal properties of natural tooth structures as well as exhibiting different mechanical properties than natural dentin (elastic modulus: ~3.5 GPa vs. 18.6 GPa) and lacks the complex tubular structure affecting bonding mechanisms. The immediate post-cementation assessment does not account for long-term aging effects that significantly influence both color stability and bond durability. The loading protocol represents acute loading conditions rather than cyclic fatigue loading characteristic of clinical function. The color measurement protocol reflects laboratory conditions with standardized illumination, while clinical color perception may be influenced by variable oral environments and individual patient factors.

Based on the statistical analysis, all null hypotheses were rejected. Significant differences were observed between KATANA UTML zirconia and IPS e.max CAD lithium disilicate laminate veneers in both color change ($P < 0.0001$) and fracture resistance ($P < 0.0001$) when cemented with different protocols. Additionally, failure modes showed significant dependence on treatment protocol.

CONCLUSIONS

Within the limitations of this in vitro study, the following conclusions can be drawn:

1. Material type and cementation protocol significantly influence laminate veneer performance, with different factors dominating specific outcomes.
2. Regarding color change, all experimental groups exceeded clinically acceptable thresholds.
3. Cementation protocol emerged as the dominant factor influencing color change, with adhesive resin cement demonstrating superior color stability compared to preheated composite across both ceramic systems.
4. For fracture resistance, material selection proved to be the primary determinant of mechanical performance, with lithium disilicate consistently outperforming ultra-translucent zirconia.
5. The LH group achieved the highest fracture resistance while the ZA group demonstrated critically inadequate performance falling below the minimum clinical threshold.
6. Failure mode analysis revealed a strong correlation between bonding quality and mechanical performance.
7. No single protocol optimized all measured outcomes simultaneously, necessitating evidence-based selection based on clinical priorities.

REFERENCES

- Abdel-Nabi, W., Ghazy, M., & Dawood, L. (2020). Fracture resistance and marginal adaptation of CAD/CAM generated monolithic zirconia laminate veneers: In-vitro study. *Mansoura Journal of Dentistry*, 6(20), 81-85.
- Aldafeeri, H. R., Abd, W., Al-Zordk, E. G., & Ghazy, M. H. (2019). Marginal accuracy of machinable monolithic zirconia laminate veneers. *IOSR Journal of Dental and Medical Sciences*, 18, 67-74.
- Al-Ali, A. M. A. H., Khalifa, N., Hadj-Hamou, A., Sheela, S., & El-Damanhoury, H. M. (2023). Effect of thickness and bonding technique on fatigue and fracture resistance of feldspathic ultra-thin laminate veneers. *European Journal of Dentistry*, 17(2), 431-438.
- Araujo, E., & Perdigão, J. (2021). Anterior veneer restorations - An evidence-based minimal-intervention perspective. *Journal of Esthetic and Restorative Dentistry*, 33(2), 296-308.
- Beier, U. S., Kapferer, I., Burtscher, D., & Dumfahrt, H. (2012). Clinical performance of porcelain laminate veneers for up to 20 years. *International Journal of Prosthodontics*, 25(1), 79-85.
- Blalock, J. S., Holmes, R. G., & Rueggeberg, F. A. (2006). Effect of temperature on unpolymerized composite resin film thickness. *Journal of Prosthetic Dentistry*, 96(6), 424-432.
- Bomicke, W., Rammelsberg, P., Stober, T., & Schmitter, M. (2017). Short-term prospective clinical evaluation of monolithic and partially veneered zirconia single crowns. *Journal of Esthetic and Restorative Dentistry*, 29(1), 22-30.
- Burke, F. J. (2012). Survival rates for porcelain laminate veneers with special reference to the effect of preparation in dentin: A literature review. *Journal of Esthetic and Restorative Dentistry*, 24(4), 257-265.
- Caminha, L. I., Dors, M., Isolan, C. P., Barbon, F. J., & Boscato, N. (2022). Effect of preheated composite resin luting agents on the color of ceramic laminates. *General Dentistry*, 70(5), 67-73.
- Chen, X. D., Hong, G., Xing, W. Z., & Wang, Y. N. (2015). The influence of resin cements on the final color of ceramic veneers. *Journal of Prosthodontic Research*, 59(3), 172-177.
- Chen, Z., Zhou, Y., Li, D., Wang, H., Jiang, L., & Zhu, L. (2024). Does the internal surface treatment technique for enhanced bonding affect the color, transparency, and surface roughness of ultra-transparent zirconia? *Clinical Oral Investigations*, 28(8), 473.

- Coelho, N. F., Barbon, F. J., Machado, R. G., Boscato, N., & Moraes, R. R. (2017). Effect of luting agent on the load to failure and accelerated-fatigue resistance of lithium disilicate laminate veneers. *Journal of Dentistry*, 67, 24-29.
- Coldea, A., Swain, M. V., & Thiel, N. (2013). Mechanical properties of polymer-infiltrated-ceramic-network materials. *Dental Materials*, 29(4), 419-426.
- Conrad, H. J., Seong, W. J., & Pesun, I. J. (2007). Current ceramic materials and systems with clinical recommendations: A systematic review. *Journal of Prosthetic Dentistry*, 98(5), 389-404.
- Daronch, M., Rueggeberg, F. A., & De Goes, M. F. (2005). Monomer conversion of pre-heated composite. *Journal of Dental Research*, 84(7), 663-667.
- Deb, S., Di Silvio, L., Mackler, H. E., & Millar, B. J. (2011). Pre-warming of dental composites. *Dental Materials*, 27(4), e51-59.
- Dumfahrt, H., & Schäffer, H. (2000). Porcelain laminate veneers. A retrospective evaluation after 1 to 10 years of service: Part II—Clinical results. *International Journal of Prosthodontics*, 13(1), 9-18.
- El Sayed, S. M., Basheer, R. R., & Bahgat, S. F. (2016). Color stability and fracture resistance of laminate veneers using different restorative materials and techniques. *Egyptian Dental Journal*, 62(1), 15.
- Fasbinder, D. J., Dennison, J. B., Heys, D., & Neiva, G. (2010). A clinical evaluation of chairside lithium disilicate CAD/CAM crowns: A two-year report. *Journal of the American Dental Association*, 141(Suppl 2), 10S-14S.
- Fróes-Salgado, N. R., Silva, L. M., Kawano, Y., Francci, C., Reis, A., & Loguercio, A. D. (2010). Composite pre-heating: Effects on marginal adaptation, degree of conversion and mechanical properties. *Dental Materials*, 26(9), 908-914.
- Ghinea, R., Perez, M. M., Herrera, L. J., Rivas, M. J., Yebra, A., & Paravina, R. D. (2010). Color difference thresholds in dental ceramics. *Journal of Dentistry*, 38(Suppl 2), e57-64.
- Gracis, S., Thompson, V. P., Ferencz, J. L., Silva, N. R., & Bonfante, E. A. (2015). A new classification system for all-ceramic and ceramic-like restorative materials. *International Journal of Prosthodontics*, 28(3), 227-235.
- Guess, P. C., Zhang, Y., Kim, J. W., Rekow, E. D., & Thompson, V. P. (2010). Damage and reliability of Y-TZP after cementation surface treatment. *Journal of Dental Research*, 89(6), 592-596.
- Gürdal, I., Atay, A., Eichberger, M., Cal, E., Üsümez, A., & Stawarczyk, B. (2018). Color change of CAD-CAM materials and composite resin cements after thermocycling. *Journal of Prosthetic Dentistry*, 120(4), 546-552.
- Harada, K., Raigrodski, A. J., Chung, K. H., Flinn, B. D., Dogan, S., & Mancl, L. A. (2016). A comparative evaluation of the translucency of zirconias and lithium disilicate for monolithic restorations. *Journal of Prosthetic Dentistry*, 116(2), 257-263.
- Hoorizad, M., Valizadeh, S., Heshmat, H., Tabatabaei, S. F., & Shakeri, T. (2021). Influence of resin cement on color stability of ceramic veneers: In vitro study. *Biomaterials Investigation in Dentistry*, 8(1), 11-17.
- Johnston, W. M. (2009). Color measurement in dentistry. *Journal of Dentistry*, 37(Suppl 1), e2-6.
- Kandil, B. S. M., Hamdy, A. M., Aboelfadl, A. K., & El-Anwar, M. I. (2019). Effect of ceramic translucency and luting cement shade on the color masking ability of laminate veneers. *Dental Research Journal*, 16(3), 192-199.
- Kwon, S. J., Lawson, N. C., McLaren, E. E., Nejat, A. H., & Burgess, J. O. (2018). Comparison of the mechanical properties of translucent zirconia and lithium disilicate. *Journal of Prosthetic Dentistry*, 120(1), 132-137.
- Layton, D. M., & Clarke, M. (2013). A systematic review and meta-analysis of the survival of non-feldspathic porcelain veneers over 5 and 10 years. *International Journal of Prosthodontics*, 26(2), 111-124.
- Le, M., Larsson, C., & Papia, E. (2019). Bond strength between MDP-based cement and translucent zirconia. *Dental Materials Journal*, 38(3), 480-489.
- Li, R., Ma, S., Zang, C., Zhang, W., Chen, Z., Ma, D., Chen, Y., & Zhang, Y. (2024). Bonding effectiveness between zirconia and resin cement: A systematic review and meta-analysis of in vitro studies. *Journal of Prosthetic Dentistry*, 131(2), 283-297.
- Liu, J. F., Yang, C. C., Luo, J. L., Liu, Y. C., Yan, M., & Ding, S. J. (2022). Bond strength of self-adhesive resin cements to a high transparency zirconia crown and dentin. *Journal of Dental Sciences*, 17(2), 973-983.
- Malallah, H. M., & Hasan, R. H. (2022). Effect of different veneering materials and techniques on fracture resistance of laminate veneers. *Baghdad College of Dentistry Journal*, 34(1), 34-40.
- Marcondes, R. L., Moraes, R. R., Pereira, J., & de Carvalho, M. A. (2021). Ceramic laminate veneers luted with

- preheated resin composite: A 10-year clinical report. *International Journal of Periodontics and Restorative Dentistry*, 41(6), 823-829.
- Miyazaki, T., Hotta, Y., Kunii, J., Kuriyama, S., & Tamaki, Y. (2009). A review of dental CAD/CAM: Current status and future perspectives from 20 years of experience. *Dental Materials Journal*, 28(1), 44-56.
 - Monteiro, J., Oliani, M., & Guilardi, L. (2018). Fatigue failure load of zirconia-reinforced lithium silicate glass ceramic cemented to a dentin analogue: Effect of etching time and hydrofluoric acid concentration. *Journal of the Mechanical Behavior of Biomedical Materials*, 77, 375-382.
 - Mundim, F. M., Garcia, L. F., & Pires-de-Souza, F. C. (2010). Effect of staining solutions and repolishing on color stability of direct composites. *Journal of Applied Oral Science*, 18(3), 249-254.
 - Paravina, R. D., Ghinea, R., Herrera, L. J., Bona, A. D., Igiel, C., Linninger, M., Sakai, M., Takahashi, H., Tashkandi, E., & Perez, M. D. M. (2015). Color difference thresholds in dentistry. *Journal of Esthetic and Restorative Dentistry*, 27(Suppl 1), S1-9.
 - Peumans, M., Van Meerbeek, B., Lambrechts, P., & Vanherle, G. (2000). Porcelain veneers: A review of the literature. *Journal of Dentistry*, 28(3), 163-177.
 - Pissai, J. F., Guanaes, B. K. A., Kintopp, C. C. A., Correr, G. M., da Cunha, L. F., & Gonzaga, C. C. (2019). Color stability of ceramic veneers as a function of resin cement curing mode and shade: 3-year follow-up. *PLoS One*, 14(7), e0219183.
 - Ramos, A. B., Murillo-Gómez, F., Arana-Correa, B. E., Goes, M. F., Rueggeberg, F. A., & de Oliveira Amaral, C. M. (2022). Effect of hydrofluoric acid concentration and etching time on the adhesive and mechanical behavior of glass-ceramics: A systematic review and meta-analysis. *Journal of Prosthetic Dentistry*, 128(4), 710-721.
 - Raposo, C. C., Ferreira, P. V. C., Nery, L. M. S., Maciel, B. M., Ardenghi, D. M., Bauer, J., & Lima, D. M. (2024). Preheated composite resins versus luting cement: Degree of conversion, film thickness, color stability and bond strength to enamel and ceramic veneers. *International Journal of Adhesion and Adhesives*, 136, 103874.
 - Rickman, L. J., Padipatvuthikul, P., & Satterthwaite, J. D. (2011). Contemporary composite resins: Part 2. *Journal of Dentistry*, 39(1), 25-32.
 - Rosentritt, M., Sawaljanow, A., Behr, M., Kolbeck, C., & Preis, V. (2015). Effect of tooth brush abrasion and thermo-mechanical loading on direct and indirect veneer restorations. *Clinical Oral Investigations*, 19, 53-60.
 - Saati, K., Valizadeh, S., Anaraki, S. N., & Moosavi, N. (2021). Effect of aging on color stability of amine-free resin cement through the ceramic laminate veneer. *Dental Research Journal*, 18, 99.
 - Soares, C. J., Soares, P. V., Pereira, J. C., & Fonseca, R. B. (2005). Surface treatment protocols in the cementation process of ceramic and laboratory-processed composite restorations: A literature review. *Journal of Esthetic and Restorative Dentistry*, 17(4), 224-235.
 - Thompson, J. Y., Stoner, B. R., Piascik, J. R., & Smith, R. (2011). Adhesion/cementation to zirconia and other non-silicate ceramics: Where are we now? *Dental Materials*, 27(1), 71-82.
 - Turgut, S., & Bagis, B. (2011). Colour stability of laminate veneers: An in vitro study. *Journal of Dentistry*, 39(Suppl 3), e57-64.
 - Van Meerbeek, B., Peumans, M., Poitevin, A., Mine, A., Van Ende, A., Neves, A., & De Munck, J. (2010). Relationship between bond-strength tests and clinical outcomes. *Dental Materials*, 26(2), e100-121.
 - Vichi, A., Louca, C., Corciolani, G., & Ferrari, M. (2020). Color related to ceramic and zirconia restorations: A review. *Dental Materials*, 36(6), 720-744.
 - Vichi, A., Fabian Fonzar, R., Carrabba, M., Louca, C., Scotti, N., Mazzitelli, C., Breschi, L., & Goracci, C. (2021). Comparison between hydrofluoric acid and single-component primer as conditioners on resin cement adhesion to lithium silicate and lithium disilicate glass ceramics. *Materials*, 14(22), 6776.
 - Yıldız, P., Ünlü, D. G., & Aydoğdu, H. M. (2024). Evaluation of vertical marginal discrepancy and load-to-failure of monolithic zirconia and lithium disilicate laminate veneers manufactured in different thicknesses. *BMC Oral Health*, 24, 913.
 - Yilmaz, B., Özçelik, T. B., & Wee, A. G. (2012). Color stability of ceramic laminate veneers cemented with self-adhesive cements after accelerated aging. *Dental Research Journal*, 9(2), 195-200.
 - Zarone, F., di Mauro, M. I., Ausiello, P., Ruggiero, G., & Sorrentino, R. (2019). Current status on lithium disilicate and zirconia: A narrative review. *BMC Oral Health*, 19(1), 134.
 - Zhang, F., Reveron, H., Spies, B. C., Van Meerbeek, B., & Chevalier, J. (2019). Trade-off between fracture resistance and translucency of zirconia and lithium-disilicate glass ceramics for monolithic restorations. *Acta Biomaterialia*, 91, 24-34.
 - Zhang, Y., & Lawn, B. R. (2018). Novel zirconia materials in dentistry. *Journal of Dental Research*, 97(2), 140-147.